JOC Article
pubs.acs.org/joc

Stereomutation of Axially Chiral Aryl Coumarins

Lodovico Lunazzi,[†] Michele Mancinelli,[†] Andrea Mazzanti,*[,†] and Marco Pierini[‡]

[†]*Department of Organic Chemistry "A. Mangini", University of Bologna, Viale Risorgimento 4, Bologna 40136, Italy, and* [‡]*Dipartimento di Studi di Chimica e Tecnologia delle Sostanze Biologicamente Attive, Università "La Sapienza", Piazzale A. Moro, 5, Roma, Italy*

mazzand@ms.fci.unibo.it

Received June 28, 2010

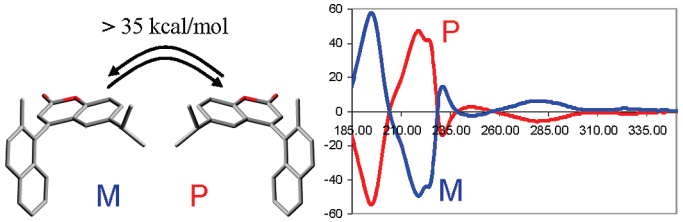

Coumarins substituted by an aryl group in position 4 display restricted rotation about the Ar−C4 bond, giving rise to conformational or configurational enantiomers (atropisomers) when such a restricted motion leads to a C_1 symmetry. The dynamics of the stereomutation processes of these axial enantiomers was monitored by dynamic NMR, dynamic enantioselective HPLC, or racemization kinetics, depending on the activation energies involved. These results were further supported by DFT computations. In the two cases where the enantiomers were sufficiently long living as to be physically separated at ambient temperature, the absolute configuration was determined by means of a theoretical simulation of their electronic circular dicroism spectra (ECD).

Introduction

Coumarin derivatives are present in a variety of naturally occurring substances:[1] they display interesting and useful biological properties in that they can behave as cytotoxic,[2] antibacterial,[3] and antimalarial[4] agents. Coumarin is also used in the pharmaceutical industry as a precursor for the synthesis of a number of synthetic anticoagulants.[5] For these reasons a number of syntheses for these types of derivatives were obtained and, in particular, the preparation of aryl coumarins has received considerable attention in the past few years.[6] A quite useful approach for the synthesis of this class of molecules has been recently reported.[7]

SCHEME 1. Structure of Compounds 1−7[a]

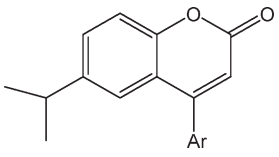

[a]Ar = 3-methylphenyl (**1**), 2-methylphenyl (**2**), 2-ethylphenyl (**3**), 2,3-dimethylphenyl (**4**), 1-naphthyl (**5**), 2-isopropylphenyl (**6**), 2-methyl-1-naphthyl (**7**).

We considered that 4-aryl coumarins might, in principle, exhibit restricted rotation about the bond joining the carbon in position 4 with a conveniently substituted aryl group. Depending on the size of the aryl substituent, such a chirality axis might generate either conformationally mobile or configurationally stable enantiomers (atropisomers). The latter, possibly, could be useful compounds for applications in asymmetric synthesis, or as precursors for the preparation

(1) Murray, R. D. H. *Nat. Prod. Rep.* **1995**, *12*, 477–505. Estévez-Braun, A. S.; González, A. G. *Nat. Prod. Rep.* **1997**, *13*, 465–475.
(2) Guilet, D.; Hélesbeux, J.-J.; Séraphin, D.; Sévenet, T.; Richomme, P.; Bruneton, J. *J. Nat. Prod.* **2001**, *64*, 563–568.
(3) Verotta, L.; Lovaglio, E.; Vidari, G.; Vita-Finzi, P.; Neri, M. G.; Raimondi, S.; Parapini, S.; Taramelli, D.; Riva, A.; Bombardelli, E. *Phytochemistry* **2004**, *65*, 2867–2879.
(4) Argotte-Ramos, R.; Ramírez-Avila, G.; Rodríguez-Gutiérrez, M. d. C.; Ovilla-Muñoz, M.; Lanz-Mendoza, H.; Rodríguez, M. H.; González-Cortazar, M.; Alvarez, L. *J. Nat. Prod.* **2006**, *69*, 1442–1444.
(5) *Coumarins: Biology, Applications, and Mode of Action*; O'Kennedy, R., Thornes, R. D., Eds.; Wiley: Weinheim, Germany, 1997.
(6) Jia, P.; Piao, D.; Oymada, J.; Lu, W.; Kitamura, T.; Fujivara, Y. *Science* **2000**, *287*, 1992–1995. Shi, Z.; He, C. *J. Org. Chem.* **2004**, *69*, 3669–3671. Li, K.; Zeng, Y.; Neuenswander, B.; Tunge *J. Org. Chem.* **2005**, *70*, 6515–6518. Oyamada, J. A.; Kitamura, T. *Tetrahedron* **2006**, *62*, 6916–6925.
(7) (a) Yamamoto, Y.; Kirai, N. *Org. Lett.* **2008**, *10*, 5513–5516. (b) Rao, M. L. N.; Venkatesh, V.; Jadhav, D. N. *Eur. J. Org. Chem.* **2010**, 3945–3955.

DOI: 10.1021/jo101261k Published on Web 08/10/2010

TABLE 1. Experimental and DFT Computed Barriers (kcal mol^{-1}) for the Rotation Process Leading to the Enantiomer Interconversion

compd	method	exptl[a]	computed[b]
1	DNMR	10.0	11.0
2	DNMR	20.1	18.9
3	DNMR	21.8	20.1
4	DHPLC	21.5	20.4
5	DHPLC	21.7	20.6
6	racemization (+24 °C) (enantiomerization)	23.4 (23.8)	22.0
7	racemization (+120 °C) (enantiomerization)	> 35	35.7

[a]Within the errors the experimental $\Delta G^{\ddagger}$ values are temperature independent, so the $\Delta S^{\ddagger}$ is negligible, see the Experimental Section. [b]The reported values refer to the enantiomerization process.

of biologically active atropisomers.[8] Accordingly we synthesized compounds **1**−**7** (Scheme 1) in which an isopropyl group was inserted in the coumarin moiety to act as a probe for the NMR detection of the molecular asymmetry.[9]

Results and Discussion

In compound **1**, which bears a *m*-tolyl substituent in position 4, the ^{13}C single line of the isopropyl methyl groups broadens on cooling and eventually splits into a pair of equally intense lines, separated by 0.05 ppm, below −80 °C. The line shape simulation yields the rate constants reported in Figure S-1 of the Supporting Information: from these values a free energy of activation ($\Delta G^{\ddagger}$) of 10.0 kcal mol^{-1} was derived (Table 1). The fact that the isopropyl methyls appear diastereotopic at low temperature indicates that the molecule adopts an asymmetric (thus chiral) conformation, implying the existence of two conformational enantiomers that interconvert with the above-mentioned barrier.

DFT calculations[10](at the B3LYP/6-31G(d) level) actually show that compound **1** adopts a twisted conformation.[11] Such a situation gives rise to two enantiomeric forms that exchange via transition states where the coumarin and the *m*-tolyl rings are essentially coplanar. There are two such transition states: one has the tolyl methyl anti, the other has the methyl syn to the C═O moiety. With respect to the ground state their computed relative energies are essentially equal (11.2 and 11.1 kcal mol^{-1}, respectively). These values match satisfactorily the experiment, the difference being only 1 kcal mol^{-1} (Table 1). In Figure S-2 of the Supporting Information are displayed the ground and transition states of these conformational enantiomers, as obtained by DFT calculations.

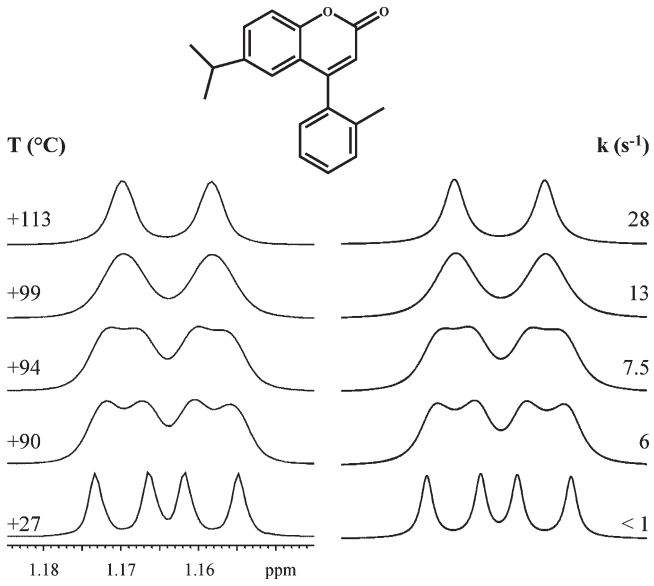

FIGURE 1. Left: Temperature dependence of the ^{1}H signals of the methyl isopropyl group of **2** (600 MHz in $C_2D_2Cl_4$). Right: Computer simulation obtained with the rate constants reported.

In compound **2**, where there is an *o*-tolyl group bonded to position 4 of coumarin, the isopropyl methyls display anisochronous signals even at ambient temperature. As shown in Figure 1 the ^{1}H spectrum displays two doublets that coalesce into a single doublet at high temperature. This implies that the two enantiomers of **2** can be detected at ambient temperature and this is confirmed by the spectrum obtained in a chiral environment, where it is shown (Figure S-3 of the Supporting Information) that the single line of the *o*-methyl group splits into two on addition of an enantiopure Pirkle's alcohol.[12] Line shape simulation of the temperature-dependent isopropyl methyl signals (Figure 1) affords a barrier of 20.1 kcal mol^{-1} (Table 1).

DFT computations predict that in the ground state of **2** the *o*-tolyl ring is essentially orthogonal to the plane of coumarin (the corresponding dihedral angle is 77°). Due to the steric hindrance exerted by the hydrogen in position 5 of the coumarin ring, the transition state where the tolyl *o*-methyl is anti to C═O has a relative computed energy much higher than when it is syn, the two values being 26.8 and 18.9 kcal mol^{-1}, respectively. The latter thus corresponds to the pathway followed by the interconversion process because this barrier not only is lower than the other but it is also much closer to the experimental value.

An analogous result was obtained in the case of **3**, where the presence of an *o*-ethyl, rather than an *o*-methyl substituent

(8) Cano, C.; Golding, B. T.; Haggerty, K.; Hardcastle, I. R.; Peacock, M.; Griffin, R. J. *Org. Biomol. Chem.* **2010**, *8*, 1922–1928.

(9) (a) Mislow, K.; Raban, M. *Top. Stereochem.* **1967**, *1*, 1. (b) Jennings, W. B. *Chem. Rev.* **1975**, *75*, 307. (c) Eliel, E. L. *J. Chem. Educ.* **1980**, *57*, 52. (d) Casarini, D.; Lunazzi, L.; Macciantelli, D. *J. Chem. Soc., Perkin Trans. 2* **1992**, 1363–1370.

(10) Frisch, M. J.; Trucks, G. W.; Schlegel, H. B.; Scuseria, G. E.; Robb, M. A.; Cheeseman, J. R.; Montgomery, J. A., Jr.; Vreven, T.; Kudin, K. N.; Burant, J. C.; Millam, J. M.; Iyengar, S. S.; Tomasi, J.; Barone, V.; Mennucci, B.; Cossi, M.; Scalmani, G.; Rega, N.; Petersson, G. A.; Nakatsuji, H.; Hada, M.; Ehara, M.; Toyota, K.; Fukuda, R.; Hasegawa, J.; Ishida, M.; Nakajima, T.; Honda, Y.; Kitao, O.; Nakai, H.; Klene, M.; Li, X.; Knox, J. E.; Hratchian, H. P.; Cross, J. B.; Bakken, V.; Adamo, C.; Jaramillo, J.; Gomperts, R.; Stratmann, R. E.; Yazyev, O.; Austin, A. J.; Cammi, R.; Pomelli, C.; Ochterski, J. W.; Ayala, P. Y.; Morokuma, K.; Voth, G. A.; Salvador, P.; Dannenberg, J. J.; Zakrzewski, V. G.; Dapprich, S.; Daniels, A. D.; Strain, M. C.; Farkas, O.; Malick, D. K.; Rabuck, A. D.; Raghavachari, K.; Foresman, J. B.; Ortiz, J. V.; Cui, Q.; Baboul, A. G.; Clifford, S.; Cioslowski, J.; Stefanov, B. B.; Liu, G.; Liashenko, A.; Piskorz, P.; Komaromi, I.; Martin, R. L.; Fox, D. J.; Keith, T.; Al-Laham, M. A.; Peng, C. Y.; Nanayakkara, A.; Challacombe, M.; Gill, P. M. W.; Johnson, B.; Chen, W.; Wong, M. W.; Gonzalez, C.; Pople, J. A. *Gaussian 03*, Revision E.01; Gaussian, Inc., Wallingford, CT, 2004.

(11) Actually there are two such twisted conformations (see Figure S-2 of the Supporting Information), with essentially the same energy: one has the tolyl methyl syn to C═O (dihedral angle = 53°), the other anti to C═O (dihedral angle = 127°). They exchange through a transition state where the coumarin and the *m*-tolyl planes are essentially orthogonal: the corresponding barrier (sometimes referred to as π-barrier) is very low (about 2 kcal mol^{-1}). This exchange process is therefore extremely fast and does not affect the variable-temperature NMR spectrum.

(12) Use was made of the enantiopure *R*-(−)-2,2,2-trifluoro-1-(9-anthryl)-ethanol (see: Pirkle, W. H.; Sikkenga, D. L.; Pavlin, M. S. *J. Org. Chem.* **1977**, *42*, 384–387.) in a 10:1 molar excess with respect to compound **2**.

in the phenyl ring increases the interconversion barrier ($\Delta G^{\ddagger} = 21.8$ kcal mol^{-1}, as in Table 1).

Introduction of a second methyl group in the meta position of compound **2** yields derivative **4**, which shows a quite noticeable buttressing effect.[13] In fact the rotation barrier interconverting the enantiomers has become much higher than in the case of **2**, so that the effects of the exchange process were not NMR visible, even at the highest attainable temperature (+120 °C).[14] According to DFT calculations this barrier is expected to be 20.4 kcal mol^{-1}, a value that is 1.5 kcal mol^{-1} higher than that computed for **2** (see Table 1): this difference thus represents the theoretical evaluation of the buttressing effect. Taking into account the experimental values observed for **2** (20.1 kcal/mol), the additional contribution of the buttressing effect should raise the barrier to a value of about 21.6 kcal mol^{-1}. Such a relatively high barrier might suggest that a physical separation of the two enantiomeric forms of **4** might be achieved.

An enantioselective HPLC experiment, however, showed that the rate interconverting the two enantiomers is such as to give the typical traces of an "in column" exchange process (i.e., dynamic HPLC effect).[15] As displayed in Figure 2 simulations of these traces (see the Experimental Section) at different temperatures yield the rate constants for the enantiomerization, from which the corresponding barrier (that could not be determined by DNMR) was obtained ($\Delta G^{\ddagger} = 21.5$ kcal mol^{-1}, as in Table 1). The difference between this experimental barrier and that of **2** is 1.4 kcal mol^{-1}, in good agreement with the DFT estimation of the buttressing effect (1.5 kcal mol^{-1}).

The naphthalene derivative **5** displays similar behavior to that of **4** in that the interconversion barrier could not be determined by dynamic NMR[14] and the variable-temperature enantioselective HPLC experiment showed again the traces typical for an "in column" interconversion in the ambient temperature range. The corresponding simulation of the dynamic HPLC traces (Figure S-4 of the Supporting Information) afforded a barrier of 21.7 kcal mol^{-1}.

In the case of compound **6** the bulkiness of the isopropyl group in the ortho position of the phenyl ring makes the enantiomers sufficiently long living as to allow their physical separation by means of an enantioselective semipreparative HPLC column (Figure 3, top).

The Electronic Circular Dichroism (ECD) spectra of the two enantiomers showed the expected opposite phased

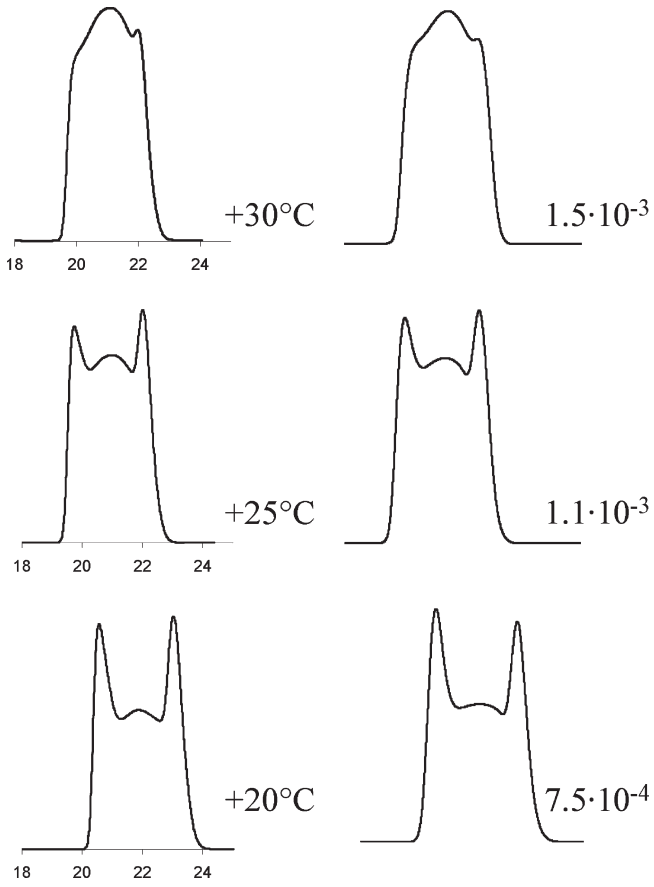

FIGURE 2. Temperature-dependent chromatograms of **4** on an enantioselective HPLC column. Experimental profiles (left, with the time scale in minutes) vs profiles (right) calculated on the basis of the best fit rate constants (k, in s^{-1}) for enantiomerization.

traces: that of the first eluted enantiomer is displayed at the bottom of Figure 3. Two conformations (**a** and **b**), differing by the orientation of the isopropyl group bonded to coumarin,[16] were optimized at the B3LYP/6-31G(d) level,[10] and the harmonic vibrational frequencies of each conformation were calculated at the same level to confirm their stability (no imaginary frequencies observed), and to evaluate the corresponding free energies. After DFT minimization, the free energies of the two conformations were found essentially equal, as shown in Figure S-5 of the Supporting Information (top).

Calculations of the ECD spectrum of both conformers were then carried out using the TD-DFT method[17] at the B3LYP/6-311++G(2d,p)//B3LYP/6-31G(d) level, and assuming the absolute configuration M (Figure S-5 of the Supporting Information, bottom). The final simulated spectrum

(13) (a) Westheimer, F. H. In *Steric Effects in Organic Chemistry*; Newman, M. S., Ed.; John Wiley and Sons, Inc.: New York, 1956; Chapter 12. (b) Karnes, H. A.; Rose, M. L.; Collat, J. W.; Newman, M. S. *J. Am. Chem. Soc.* **1968**, *90*, 458–461. (c) Decouzon, M.; Ertl, P.; Exner, O.; Gal, J.-F.; Maria, P.-C. *J. Am. Chem. Soc.* **1993**, *115*, 12071–12078. (d) Heiss, F.; Marzi, E.; Schlosser, M. *Eur. J. Org. Chem.* **2003**, 4625–4629. (e) Gorecka, J.; Heiss, C.; Scopelliti, R.; Schlosser, M. *Org. Lett.* **2004**, *6*, 4591–4593. (f) Heiss, C.; Leroux, F.; Schlosser, M. *Eur. J. Org. Chem.* **2005**, 5242–5247. (g) Schlosser, M.; Cottet, F.; Heiss, C.; Lefebvre, O.; Marull, M.; Masson, E.; Scopelliti, R. *Eur. J. Org. Chem.* **2006**, 729–734. (h) Lunazzi, L.; Mancinelli, M.; Mazzanti, A. *J. Org. Chem.* **2008**, *73*, 2198–2205.

(14) This was due to the fact that the chemical shift separation of the isopropyl methyl signals was exceedingly small in the solvents required to reach the high temperatures. For the same reason, even a high-temperature EXSY NMR experiment (see: Sanders, J. K. M.; Hunter, B. H. *Modern NMR Spectroscopy*, 2nd ed.; Oxford University Press: Oxford, UK, 1993; p 226.) did not allow us to observe the effects of this exchange process.

(15) (a) Gasparrini, F.; Grilli, S.; Leardini, R.; Lunazzi, L.; Mazzanti, A.; Nanni, D.; Pierini, M.; Pinamonti, M. *J. Org. Chem.* **2002**, *67*, 3089–3095. (b) Ciogli, A.; Dalla Cort, A.; Gasparrini, F.; Lunazzi, L.; Mandolini, L.; Mazzanti, A.; Pasquini, C.; Pierini, M.; Schiaffino, L.; Mihan, F. Y. *J. Org. Chem.* **2008**, *73*, 6108–6118. (c) Wolf, C. *Dynamic Stereochemistry of Chiral Compounds*; RCS Publishing: Cambridge, UK, 2008; Chapter 4, pp 136−179.

(16) Other possible conformers were found to have energies too high to be significantly populated and were therefore neglected.

(17) Mazzeo, G.; Giorgio, E.; Zanasi, R.; Berova, N.; Rosini, C. *J. Org. Chem.* **2010**, *75*, 4600–4603. Pescitelli, G.; Di Pietro, S.; Cardellicchio, C.; Annunziata, M.; Capozzi, M.; Di Bari, L. *J. Org. Chem.* **2010**, *75*, 1143–1154. Jacquemin, D.; Perpète, E. A.; Ciofini, I.; Adamo, C.; Valero, R.; Zhao, Y.; Truhlar, D. G. *J. Chem. Theory Comput.* **2010**, *6*, 2071–2085. Gioia, C.; Fini, F.; Mazzanti, A.; Bernardi, L.; Ricci, A. *J. Am. Chem. Soc.* **2009**, *131*, 9614–9615. Stephens, P. J.; Pan, J. J.; Devlin, F. J.; Cheeseman, J. R. *J. Nat. Prod.* **2008**, *71*, 285–288. For reviews see: Bringmann, G.; Bruhn, T.; Maksimenka, K.; Hemberger, Y. *Eur. J. Org. Chem.* **2009**, 2717–2727. Bringmann, G.; Gulder, T. A. M.; Reichert, M.; Gulder, T. *Chirality* **2008**, *20*, 628–642. Berova, N.; Di Bari, L.; Pescitelli, G. *Chem. Soc. Rev.* **2007**, *36*, 914.

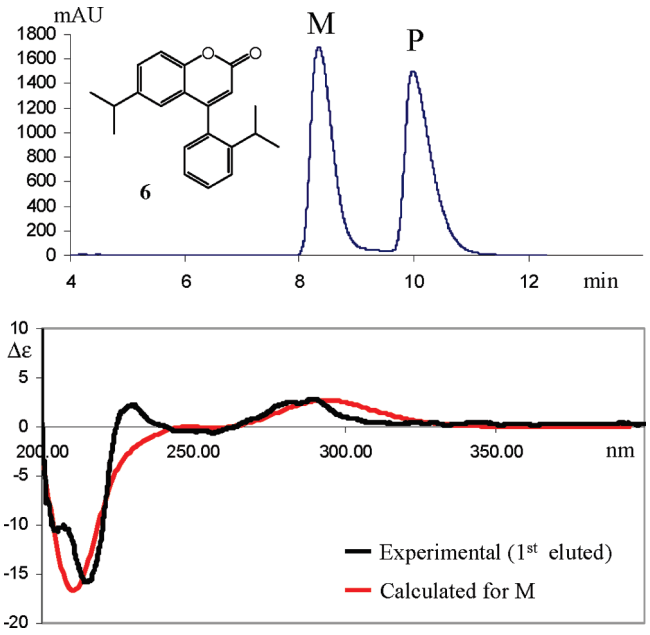

FIGURE 3. Top: Chromatogram of compound **6** on an enantioselective HPLC column. Bottom: Calculated (red) and experimental (black) ECD spectrum of the first eluted enantiomer in the same solvent mixture used for the separation.

(Figure 3, bottom) was obtained taking into account the 52:48 population ratio determined from the calculated free energies at the B3LYP/6-31G(d) level, and assuming Boltzmann statistics. The satisfactory agreement between the calculated and the experimental ECD spectrum allowed us to confidently assign the absolute configuration M to the first eluted enantiomer.

The first eluted enantiomer of **6** was then left to racemize inside the ECD spectrometer at +24 °C, and the evolution of this kinetic process was followed by the decay of the ECD signal at 216 nm. A rate constant of 3.7×10^{-5} s^{-1} was measured (Figure S-6 of the Supporting Information), from which a barrier ($\Delta G^{\ddagger}$) of 23.4 kcal mol^{-1} (Table 1) was derived for the racemization process. According to the well-known relationship existing between enantiomerization (k^e) and racemization (k^r) rate constants (i.e., $k^r = 2k^e$), the related enantiomerization process is therefore characterized by a barrier of 23.8 kcal mol^{-1}.

On the basis of the results for the 1-naphthyl derivative **5** and for compound **6**, we anticipated that compound **7**, having an even more hindered group as a substituent (i.e., 2-methyl-1-naphthyl), was likely to give rise to a pair of atropisomers configurationally stable at ambient temperature. A computed structure of **7** is reported in Figure S-7 of the Supporting Information, together with the computed transition states: the lower energy of the latter is as high as 35.7 kcal mol^{-1} (Table 1), thus supporting the prediction that these atropisomers should not be able to interconvert at ambient temperature, contrary to the cases of **5** and **6**. Both the ^1H and ^{13}C spectra show that the methyl groups of the isopropyl moiety of **7** remain diastereotopic at any attainable temperature. The two atropisomers (M and P enantiomers) were separated by means of an enantioselective HPLC column (Figure 4, top) and the corresponding ECD spectra displayed the expected opposite phased traces.

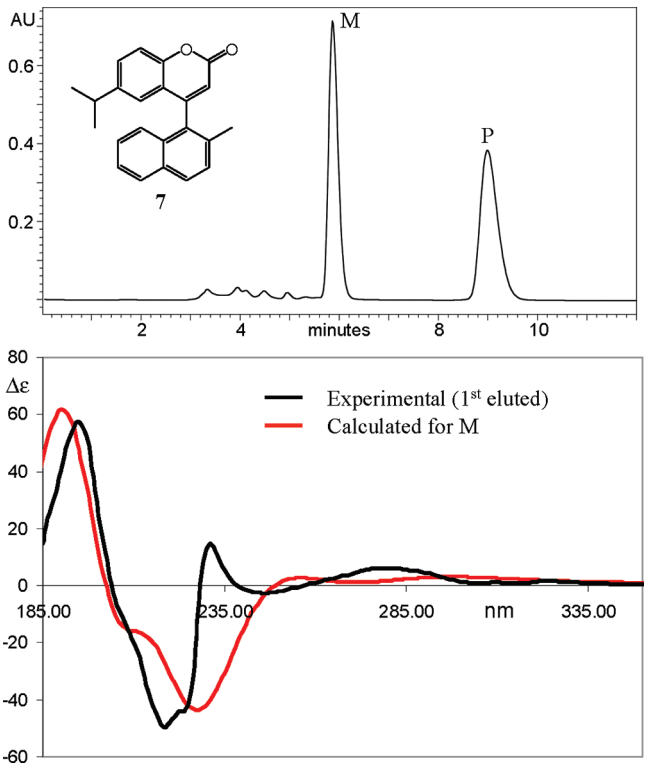

FIGURE 4. Top: Chromatogram of compound **7** on an enantioselective HPLC column. Bottom: Calculated (red) and experimental (black) ECD spectrum of the first eluted atropisomer in acetonitrile.

Theoretical simulation of these traces, performed in the same way as described for compound **6**,[16] allowed us to assign the absolute M configuration to the first eluted atropisomer (Figure 4, bottom).

The second eluted atropisomer P was kept at +120 °C in a tetrachloroethane solution for 24 h, but the subsequent enantioselective HPLC analysis did not display the appearance of the signal due to the M enantiomeric partner, thus implying[18] a barrier higher than 35 kcal mol^{-1}. This result agrees with the theoretical barrier (35.7 kcal mol^{-1}, as in Table 1) predicted for their interconversion: it can be thus concluded that the enantiomers of **7** can be considered configurationally stable atropisomers.

Experimental Section

Materials. 2-Methylphenylboronic acid, 2-ethylphenylboronic acid, 2-isopropylphenylboronic acid, 2,3-dimethylphenylboronic acid, and 1-naphthylboronic acid were commercially available. Dimethyl (2-methylnaphthalen-1-yl)boronate was prepared following known procedures.[19] 4-Arylcoumarins **1**−**7** were prepared according to the general procedure[7a] displayed in Scheme 2.

Compounds **8**,[20] **9**,[21] **10**, and **11** were prepared following a procedure described in ref 7a.

(18) After 24 h at +120 °C, the enantioselective HPLC analysis showed that the amount of the first eluted enantiomer, if present, was certainly much lower than 1%. If a 1% population is assumed, the corresponding rate constant is about 10^{-7} s^{-1}, which corresponds to a barrier of 35.5 kcal mol^{-1}. Accordingly the barrier for the racemization of **7** must be higher than 35 kcal mol^{-1}.

(19) Thompson, W. J.; Gaudino, J. *J. Org. Chem.* **1984**, *49*, 5237. Andersen, N. G.; Maddaford, S. P.; Keay, B. A. *J. Org. Chem.* **1996**, *61*, 9556–9559.

(20) Shukla, R.; Lindeman, S. V.; Rathore, R. *J. Am. Chem. Soc.* **2006**, *128*, 5328–5329.

(21) Yu, X.; Scheller, D.; Rademacher, O.; Wolff, T. *J. Org. Chem.* **2003**, *68*, 7386–7399.

SCHEME 2. Synthesis of Coumarins 1−7[a]

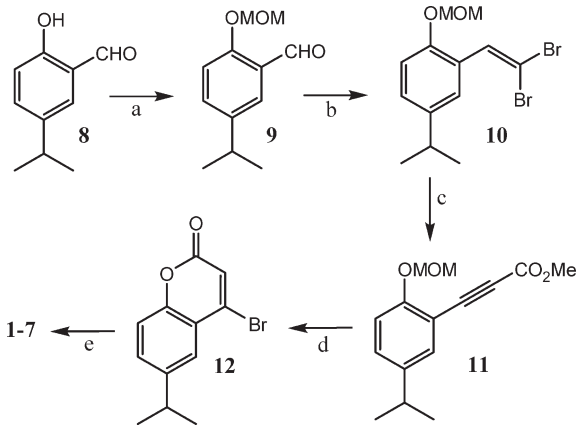

[a]Reagents and conditions: (a), *t*-BuOK, MOM-Cl, THF, 25 °C; (b) CBr_4, PPh_3, NEt_3, CH_2Cl_2, 0 °C; (c) *n*-BuLi, MeOCOCl, THF, −78 °C; (d) HBr, Et_2O, 0 °C; (e) Ar−$B(OH)_2$, $Pd(PPh_3)_4$, K_2CO_3, benzene/H_2O/EtOH, reflux.

2-(2,2-Dibromovinyl)-4-isopropyl-1-(methoxymethoxy)benzaldehyde (10): ^{1}H NMR (400 MHz, CD_3CN, 25 °C, TMS) δ 1.20 (d, 6 H, J = 6.9 Hz), 2.84 (sept, 1 H, J = 6.9 Hz), 3.42 (s, 3 H), 5.16 (s, 2 H), 7.03 (d, 1 H, J = 8.4 Hz), 7.20 (dd, 1 H, J = 2.4, 8.4 Hz), 7.50 (d, 1 H, J = 2.4), 7.63 (s, 1H); ^{13}C NMR (100.6 MHz, CD_3CN, 25 °C, TMS) δ 24.1 (CH_3), 33.9 (CH), 56.4 (CH_3), 90.2 (CH_2), 95.6 (CH), 115.5 (C_q), 127.9 (CH), 128.8 (CH), 134.7 (CH), 142.8 (C_q), 148.9 (q), 153.1 (C_q).

Methyl 3-(5-isopropyl-2-(methoxymethoxy)phenyl)propiolate (11): ^{1}H NMR (400 MHz, CD_3CN, 25 °C, TMS) δ 1.18 (d, 6 H, J = 7.0 Hz), 2.85 (sept, 1 H, J = 7.0 Hz), 3.44 (s, 3 H), 3.78 (s, 3 H), 5.23 (s, 2 H), 7.10 (d, 1 H, J = 8.8 Hz), 7.33 (dd, 1 H, J = 2.3, 8.8 Hz), 7.41 (d, 1 H, J = 2.3 Hz); ^{13}C NMR (150.8 MHz, CD_3CN, 25 °C, TMS) δ 23.9 (CH_3), 33.7 (CH), 53.3 (CH_3), 56.5 (CH_2), 84.0 (CH), 84.4 (CH), 95.8 (CH_3), 110.0 (C_q), 116.0 (C), 131.7 (CH), 133.1 (CH), 143.5 (C_q), 158.2 (COO); HRMS (EI) calcd for $C_{15}H_{18}O_4$ 262.1205, found 262.1208

4-Bromo-6-isopropyl-2*H*-cromen-2-one (12). Compound **12** was prepared following a procedure described in ref 22: ^{1}H NMR (600 MHz, $CDCl_3$, 25 °C TMS) δ 1.27 (d, 6 H, J = 7.0 Hz), 2.99 (sept, 1 H, J = 7.0 Hz), 6.79 (s, 1 H), 7.22 (d, 1 H, J = 8.5 Hz), 7.43 (dd, 1 H, J = 8.5, 1.8 Hz), 7.61 (d, 2 H, J = 1.8 Hz); ^{13}C NMR (150.8 MHz, $CDCl_3$, 25 °C TMS) δ 24.2 (2 CH_3), 33.9 (CH), 117.1 (CH), 118.78 (C_q), 119.5 (CH), 125.5 (CH), 131.9 (CH), 141.9 (C_q), 146.1 (C_q), 151.0 (C_q), 159.1 (COO); HRMS (EI) calcd for $C_{12}H_{11}O_2Br$ 265.9942, found 265.9947.

General Procedure for Compounds 1−6. To a solution of 4-bromo-6-isopropyl-2*H*-cromen-2-one (**12**) (0.053 g, 0.2 mmol, in 2 mL of benzene) were added K_2CO_3 (2 M solution, 1.0 mL), the appropriate boronic acid (0.5 mmol, suspension in 2 mL of THF), and $Pd(PPh_3)_4$ (0.046 g, 0.04 mmol) at room temperature. The stirred solution was refluxed for 2−3 h, the reaction being monitored by GC-MS. After cooling to room temperature, Et_2O and H_2O were added and the extracted organic layer was dried (Na_2SO_4) and evaporated. The crude products were purified by chromatography on silica gel (petroleum ether/Et_2O 10:1). Analytically pure samples of **1−6** were obtained by semi-preparative HPLC on a C18 column (Luna C18(2) 5 μm, 250 × 10 mm, 5 mL/min, ACN/H_2O 90/10 v/v). All the compounds are colorless oils.

6-Isopropyl-4-(*m*-tolyl)-2*H*-cromen-2-one (1): t_R = 8.76 min; ^{1}H NMR (600 MHz, $CDCl_3$, 25 °C, TMS) δ 1.21 (d, 6 H, J = 7.0 Hz), 2.46 (s, 3 H), 2.90 (sept, 1 H, J = 7.0 Hz), 6.35 (s, 1 H), 7.25−7.27 (m, 1 H), 7.31−7.36 (m, 3 H), 7.41−7.44 (m, 2 H); ^{13}C NMR (150.8 MHz, $CDCl_3$, 25 °C, TMS) δ 21.6 (CH_3), 24.2 (2 CH_3), 33.8 (CH), 115.1 (CH), 117.3 (CH), 118.9 (C_q), 124.6 (CH), 125.7 (CH), 128.8 (CH), 129.3 (CH), 130.4 (CH), 130.5 (CH), 135.5 (C_q), 138.9 (C_q), 145.0 (C_q), 152.7 (C_q), 156.1 (C_q), 161.3 (COO); HRMS (ESI-FT-ICR) calcd for $C_{19}H_{19}O_2$ [M + H]$^+$ 279.1380, found 279.1375.

6-Isopropyl-4-(*o*-tolyl)-2*H*-cromen-2-one (2): t_R = 7.77 min; ^{1}H NMR (600 MHz, $CDCl_3$, 25 °C TMS) δ 1.16 (d, 3 H, J = 7.0 Hz), 1.15 (d, 3 H J = 7.0 Hz), 2.16 (s, 3 H), 2.84 (sept, 1 H, J = 7.0 Hz), 6.30 (s, 1 H), 6.87 (d, 1 H, J = 2.1 Hz), 7.20 (dd, 1 H, J = 1.1, 7.6 Hz), 7.34 (m, 3 H), 7.40−7.43 (m, 2 H), 7.41−7.44 (m, 2 H); ^{13}C NMR (150.8 MHz, $CDCl_3$, 25 °C, TMS) δ 20.0 (CH_3), 24.0 (CH_3), 24.2 (CH_3), 33.7 (CH), 115.8 (CH), 117.2 (CH), 119.3 (C_q), 124.5 (CH), 126.3 (CH), 128.7 (CH), 129.4 (CH), 130.4 (CH), 130.7 (CH), 135.1 (C_q), 135.5 (C_q), 145.3 (C_q), 152.3 (C_q), 156.4 (C_q), 161.3 (COO); HRMS (ESI-FT-ICR) calcd for $C_{19}H_{19}O_2$ [M + H]$^+$ 279.1380, found 279.1382.

6-Isopropyl-4-(2-ethylphenyl)-2*H*-cromen-2-one (3): t_R = 9.24 min; ^{1}H NMR (600 MHz, $CDCl_3$, 25 °C, TMS) δ 1.10 (t, 3 H, J = 7.6 Hz), 1.14 (d, 3 H, J = 7.0 Hz), 1.15 (d, 3H, J = 7.0 Hz), 2.45 (m, 1 H), 2.49 (m 1 H), 2.83 (sept, 1 H, J = 7.0 Hz), 6.32 (s, 1H), 6.86 (d, 1 H, J = 2.35 Hz), 7.16 (dd, 1 H, J = 1.2, 7.6 Hz), 7.30−7.36 (m, 2 H), 7.39−7.43 (m, 2 H), 7.46−7.49 (m, 1 H); ^{13}C NMR (150.8 MHz, $CDCl_3$, 25 °C, TMS) δ 15.8 (CH_3), 24.0 (CH_3), 24.3 (CH_3), 26.4 (CH_2), 33.8 (CH), 116.0 (CH), 117.2 (CH), 119.8 (C_q), 124.6 (CH), 126.3 (CH), 128.8 (CH), 129.0 (CH), 129.6 (CH), 130.4 (CH), 134.4 (C_q), 141.8 (C_q), 145.3 (C_q), 152.3 (C_q), 156.4 (C_q), 161.3 (COO); HRMS (ESI-Exactive-Orbitrap) calcd for $C_{20}H_{21}O_2$ [M + H]$^+$ 293.1536, found 293.1532.

6-Isopropyl-4-(2,3-dimethlphenyl)-2*H*-cromen-2-one (4): t_R = 9.22 min; ^{1}H NMR (600 MHz, $CDCl_3$, 25 °C, TMS) δ 1.16 (d, 3 H, J = 7.0 Hz), 1.15 (d, 3 H, J = 7.0 Hz), 2.05 (s, 3 H), 2.38 (s, 3 H), 2.84 (sept, 1 H, J = 7.0 Hz), 6.29 (s, 1 H), 6.86 (d, 1 H, J = 2.1 Hz), 7.03 (d, 1 H, J = 7.6 Hz), 7.23 (t, 1 H, J = 7.6 Hz), 7.29 (d, 1 H, J = 7.6 Hz), 7.33 (d, 1 H, J = 8.5 Hz), 7.41 (dd, 1 H, J = 2.1, 8.5 Hz); ^{13}C NMR (150.8 MHz, $CDCl_3$, 25 °C, TMS) δ 17.2 (CH_3), 20.6 (CH_3), 24.0 (CH_3), 24.3 (CH_3), 33.7 (CH), 115.8 (CH), 117.2 (CH), 119.6 (C_q), 124.7 (CH), 126.0 (CH), 126.5 (CH), 130.2 (CH), 130.8 (CH), 134.0 (C_q), 135.2 (C_q), 137.8 (C_q), 145.2 (C_q), 152.2 (C_q), 157.1 (C_q), 161.4 (COO); HRMS (ESI-FT-ICR) calcd for $C_{20}H_{21}O_2$ [M + H]$^+$ 293.1536, found 293.1528.

6-Isopropyl-4-(naphthalene-1-yl)-2*H*-cromen-2-one (5): t_R = 8.75 min; ^{1}H NMR (600 MHz, $CDCl_3$, 25 °C, TMS) δ 1.03 (d, 3 H, J = 7.0 Hz), 1.04 (d, 3 H, J = 7.0 Hz), 2.70 (sept, 1 H, J = 7.04 Hz), 6.48 (s, 1 H), 6.82 (d, 1 H, J = 1.76 Hz), 7.36−7.62 (m, 7 H), 7.95 (d, 1 H, J = 8.2 Hz), 8.01 (d, 1 H, J = 8.2 Hz); ^{13}C NMR (150.8 MHz, $CDCl_3$, 25 °C, TMS) δ 24.0 (CH_3), 24.2 (CH_3), 33.8 (CH), 117.1 (CH), 117.4 (CH), 120.0 (C_q), 125.2 (CH), 125.6 (CH), 125.8 (CH), 126.8 (2 CH), 127.1 (CH), 128.8 (CH), 130.1 (CH), 130.6 (CH), 131.2 (C_q), 133.2 (C_q), 133.8 (C_q), 145.3 (C_q), 152.4 (C_q), 155.6 (C_q), 161.3 (COO); HRMS (ESI-Exactive-Orbitrap) calcd for $C_{22}H_{19}O_2$ [M + H]$^+$ 315.1380, found 315.1373.

6-Isopropyl-4-(2-isopropylphenyl)-2*H*-cromen-2-one (6): t_R = 10.93 min; ^{1}H NMR (600 MHz, CD_3CN, 25 °C, TMS) δ 1.107 (d, 3 H, J = 6.9 Hz), 1.123 (d, 3H, J = 6.9 Hz), 1.125 (d, 3 H, J = 6.9 Hz), 1.144 (d, 3H, J = 6.9 Hz), 2.74 (sept, 1 H, J = 6.9 Hz), 2.85 (sept, 1 H, J = 6.9 Hz), 6.29 (s, 1 H), 6.84 (d, 1 H, J = 2.3 Hz), 7.18−7.19 (m, 1 H), 7.33−7.36 (m, 2 H), 7.50−7.56 (m, 3 H); ^{13}C NMR (150.8 MHz, CD_3CN, 25 °C, TMS) δ 22.6 (CH_3), 23.2 (CH_3), 23.5 (CH_3), 24.5 (CH_3), 30.6 (CH), 33.5(CH), 116.1 (CH), 116.9 (CH), 120.1 (C_q), 124.4 (CH), 126.1 (CH), 126.3 (CH), 128.6 (CH), 129.8 (CH), 130.7 (CH), 133.9 (C_q), 145.2 (C_q), 146.7 (C_q), 152.2 (C_q), 156.2 (C_q), 160.6 (COO); HRMS (ESI-Exactive-Orbitrap) calcd for $C_{21}H_{23}O_2$ [M + H]$^+$ 307.1693, found 307.1684.

(22) Munt, S. P.; Thomas, E. J. *Chem. Commun.* **1989**, 480–482.

6-Isopropyl-4-(2-methylnaphthalene-1-yl)-2*H*-cromen-2-one (7). To a solution of 2-methylnaphthyllithium, obtained at −78 °C by the dropwise addition of butyllithium (10 mL of a 1.6 M solution in hexanes) to 1-bromo-2-methylnaphthalene (15 mmol in 40 mL of dry THF), was added $B(OMe)_3$ (15 mmol) dropwise.[19] A 1.0 mL sample of the resulting 0.5 M solution of dimethyl (2-methylnaphthalen-1-yl)boronate was then used in the coupling reaction with 4-bromo-6-isopropyl-2*H*-cromen-2-one (**12**) (0.2 mmol) and $Pd(PPh_3)_4$ (0.046 g, 0.04 mmol), following the same procedure as above. An analytically pure sample of **7** as a colorless oil was obtained by semipreparative HPLC on a C18 column (Luna C18(2) 5 μm, 250 × 10 mm, 5 mL/min, ACN/H_2O 90/10 v/v): t_R = 9.36 min; ^{1}H NMR (600 MHz, CD_3CN, 25 °C, TMS) δ 0.99 (d, 3 H, J = 7.0 Hz), 1.01 (d, 3 H, J = 7.0 Hz), 2.28 (s, 3 H), 2.70 (sept, 1 H, J = 7.0 Hz), 6.36 (s, 1 H), 6.62−6.63 (m, 1 H), 7.38−7.43 (m, 2 H), 7.48−7.57 (m, 4 H), 7.94−7.99 (m, 2 H); ^{13}C NMR (150.8 MHz, CD_3CN, 25 °C, TMS) δ 19.6 (CH_3), 23.2 (CH_3), 23.3 (CH_3), 33.3 (CH), 117.1 (CH), 117.6 (CH), 119.6 (C_q), 124.1 (CH), 125.1 (CH), 125.7 (CH), 126.9 (CH), 128.3 (CH), 128.8 (CH), 129.1 (CH), 130.6 (CH), 130.7 (C_q), 131.6 (C_q), 132.1 (C_q), 133.8 (C_q), 145.5 (C_q), 152.7 (C_q), 154.6 (C_q), 160.7 (COO); HRMS (ESI-FT-ICR) calcd for $C_{23}H_{21}O_2$ $[M + H]^+$ 329.1536, found 329.1528.

HPLC and CD Spectra. Dynamic HPLC chromatograms were obtained with use of a temperature-controlled system. DHPLC chromatograms of **4** and **5** were obtained with a Daicel Chiralcel AD-H (98:2 hexane/*i*Pr-OH) and a Phenomenex LUX amilose-2 (65:35 hexane/*i*Pr-OH), respectively. Separation of the two atropisomers of **6** was achieved at +25 °C on a Phenomenex LUX amilose-2 250 × 4.6 mm column, at a flow rate of 1.0 mL/min, using hexane/*i*Pr-OH 95:5 as eluent. Separation of the two atropisomers of **7** was achieved at +25 °C on a Daicel Chiralcel OD-H 250 × 4.6 mm column, at a flow rate of 1.0 mL/min, using hexane/*i*Pr-OH 70:30 as eluent. To have a sufficient amount to record the CD spectra, 10 injections (50 μg each) were collected. UV detection was fixed at 254 nm. UV absorption spectra were recorded at +25 °C in hexane on the racemic mixtures, in the 200−400 nm spectral region. Maximum molar absorption coefficients were recorded at 209 nm for **6** (ε = 12 150) and 226 nm for **7** (ε = 54 550). ECD spectra were recorded at +24 °C using the collected HPLC fractions (hexane/*i*Pr-OH 95:5) in the case of **6**, whereas the spectra of **7** were recorded in acetonitrile at +24 °C. The same path length of 0.2 cm was used in both cases, and spectra were recorded in the range 200−400 nm for **6** and 185−400 for **7**, respectively; reported $\Delta\varepsilon$ values are expressed as L mol^{-1} cm^{-1}.

Simulation of Dynamic Chromatograms. Simulations of variable-temperature experimental chromatograms of **4**−**5** were performed by using the homemade computer program AutoDHPLCy2k,[23] which implements both stochastic and theoretical plate models according to mathematical equations and procedures described within.[24] The involved algorithms may take into account all types of first-order interconversions, including therefore the case of enantiomerizations, as well as the chance to reproduce tailing effects. Dynamic chromatograms relevant to the enantiomerization process of compound **3** were simulated by the stochastic model, while those relevant to compound **6** were simulated by the theoretical plate model. In both cases tailing effects were taken into account. All line shape analyses were carried out by performing simplex optimization of both chromatographic and kinetic parameters, until obtaining the best agreement between experimental and simulated dynamic profiles (minimization of the root-mean-square differences, rmsd, between the compared chromatograms). Simulations were automatically stopped upon achievement of rmsd convergence (rmsd < 0.001). Errors associated to the evaluated rate constants were estimated at less than 2%.

NMR Spectroscopy. The ambient-temperature NMR spectra were obtained at 600 or 400 MHz for ^{1}H and at 150.8 or 100.6 MHz for ^{13}C. The assignments of the ^{1}H and ^{13}C signals were obtained by bidimensional experiments (edited-gHSQC[25] and gHMBC[26] sequences). The variable-temperature spectra[27] were recorded at 600 MHz for ^{1}H and 150.8 MHz for ^{13}C. Temperature calibrations were performed before the experiments, using a Cu/Ni thermocouple immersed in a dummy sample tube filled with 1,1,2,2-tetrachloroethane, and under conditions as nearly identical as possible. The uncertainty in the temperatures was estimated from the calibration curve to be ±1 °C. The line shape simulations were performed by means of a PC version of the QCPE program DNMR 6 no. 633, Indiana University, Bloomington, IN.

Calculations. Geometry optimizations were carried out at the B3LYP/6-31G(d)[28] level by means of the Gaussian 03 series of programs:[10] the standard Berny algorithm in redundant internal coordinates and default criteria of convergence were employed. The computed energies reported in Table 1 represent total electronic energies. In general, these give the best fit with experimental DNMR data.[29] Therefore, the computed numbers have not been corrected for zero-point energy contributions or other thermodynamic parameters. This avoids artifacts that might result from the inevitably ambiguous choice of an adequate reference temperature, from empirical scaling factors tuned for a better matching of experimental and theoretical numbers[30] and from the treatment of low-frequency vibration as harmonic oscillators. This is particularly important in the present case, where many calculated frequencies fall below the 500−600 cm^{-1} range.[31] Full thermochemistry-corrected data are reported in the Supporting Information. Harmonic vibrational frequencies were calculated for all the stationary points. For each optimized ground state the frequency analysis showed the absence of imaginary frequencies, whereas each transition state showed a single imaginary frequency. Visual inspection of the corresponding normal mode[32] was used to confirm that the correct transition state had been found. TD-DFT calculations were performed at the B3LYP/6-311++G(2d,p)//B3LYP/6-31G(d) level.[33] Rotational strength were calculated in both length and velocity representation. The resulting values are very similar, therefore the errors due to basis set incompleteness are very small.[34] The ECD spectra were obtained by applying a 0.5 eV Gaussian shaped line width.[32] To cover the 170−400 nm range, 70 transitions were calculated for each conformation.

Acknowledgment. L.L. and A.M. received financial support from the University of Bologna (RFO) and from MIUR, Rome (PRIN national project "Stereoselection in Organic Synthesis, Methodologies and Applications").

(23) Cirilli, R.; Costi, R.; Di Santo, R.; La Torre, F.; Pierini, M.; Siani, G. *Anal. Chem.* **2009**, *81*, 3560–3570.
(24) (a) Jung, M. *QCPE Bull.* **1992**, *12*, 52. (b) Trapp, O.; Schurig, V. *Comput. Chem.* **2001**, *25*, 187–195.
(25) Bradley, S. A.; Krishnamurthy, K. *Magn. Reson. Chem.* **2005**, *43*, 117–123. Willker, W.; Leibfritz, D.; Kerssebaum, R.; Bermel, W. *Magn. Reson. Chem.* **1993**, *31*, 287–292.
(26) Hurd, R. E.; John, B. K. *J. Magn. Reson.* **1991**, *91*, 648–653.
(27) For a recent review see: Casarini, D.; Lunazzi, L.; Mazzanti, A. *Eur. J. Org. Chem.* **2010**, 2035–2056.
(28) Becke, A. D. *J. Chem. Phys.* **1993**, *98*, 5648–5652. Lee, C.; Yang, W.; Parr, R. G. *Phys. Rev. B* **1988**, *37*, 785–789. Stephens, P. J.; Devlin, F. J.; Chabalowski, C. F.; Frisch, M. J. *J. Phys. Chem.* **1994**, *98*, 11623–11627.
(29) Ayala, P. Y.; Schlegel, H. B. *J. Chem. Phys.* **1998**, *108*, 2314–2325.
(30) Tormena, C. F.; Rittner, R.; Abraham, R. J.; Basso, E. A.; Fiorin, B. C. *J. Phys. Org. Chem.* **2004**, *17*, 42–48.
(31) Wong, M. W. *Chem. Phys. Lett.* **1996**, *256*, 391–399.
(32) Gaussview 4.1.2, Semichem Inc., 2006.
(33) The use of a moderate basis set is dictated by the molecular size and by the need of limiting the computational time (about 20−24 h on a 8-core server).
(34) Stephens, P. J.; McCann, D. M.; Devlin, F. J.; Cheeseman, J. R.; Frisch, M. J. *J. Am. Chem. Soc.* **2004**, *126*, 7514–7521.

Dr. G. Bianco, University of Basilicata, Potenza is gratefully acknowledged for the acquisition of some HRMS mass spectra.

Supporting Information Available: Variable-temperature NMR spectra of **1**, NMR spectrum of **2** in a chiral environment, computed components of the ECD spectrum of **6**, DFT computed structures of **1** and **7**, variable-temperature HPLC traces of **5**, kinetics of the enantiomerization of **6**, ^{1}H and ^{13}C NMR spectra and computational data of **1**−**7**. This material is available free of charge via the Internet at http://pubs.acs.org.